Apoptosis-Like Death, an Extreme SOS Response in *Escherichia coli*

Ariel Erental,[a] Ziva Kalderon,[a] Ann Saada,[b,c] Yoav Smith,[d] Hanna Engelberg-Kulka[a]

Department of Microbiology and Molecular Genetics, Institute for Medical Research Israel-Canada (IMRIC), The Hebrew University-Hadassah Medical School, Jerusalem, Israel[a]; Monique and Jacques Robo Department of Genetic Research[b] and Department of Genetic and Metabolic Diseases,[c] Hadassah-Hebrew University Medical Center, Jerusalem, Israel; Genomic Data Analysis Unit, The Hebrew University-Hadassah Medical School, The Hebrew University of Jerusalem, Jerusalem, Israel[d]

ABSTRACT **In bacteria, SOS is a global response to DNA damage, mediated by the *recA-lexA* genes, resulting in cell cycle arrest, DNA repair, and mutagenesis. Previously, we reported that *Escherichia coli* responds to DNA damage via another *recA-lexA*-mediated pathway resulting in programmed cell death (PCD). We called it apoptosis-like death (ALD) because it is characterized by membrane depolarization and DNA fragmentation, which are hallmarks of eukaryotic mitochondrial apoptosis. Here, we show that ALD is an extreme SOS response that occurs only under conditions of severe DNA damage. Furthermore, we found that ALD is characterized by additional hallmarks of eukaryotic mitochondrial apoptosis, including (i) rRNA degradation by the endoribonuclease YbeY, (ii) upregulation of a unique set of genes that we called extensive-damage-induced (*Edin*) genes, (iii) a decrease in the activities of complexes I and II of the electron transport chain, and (iv) the formation of high levels of $OH^{\cdot}$ through the Fenton reaction, eventually resulting in cell death. Our genetic and molecular studies on ALD provide additional insight for the evolution of mitochondria and the apoptotic pathway in eukaryotes.**

IMPORTANCE **The SOS response is the first described and the most studied bacterial response to DNA damage. It is mediated by a set of two genes, *recA-lexA*, and it results in DNA repair and thereby in the survival of the bacterial culture. We have shown that *Escherichia coli* responds to DNA damage by an additional *recA-lexA*-mediated pathway resulting in an apoptosis-like death (ALD). Apoptosis is a mode of cell death that has previously been reported only in eukaryotes. We found that *E. coli* ALD is characterized by several hallmarks of eukaryotic mitochondrial apoptosis. Altogether, our results revealed that *recA-lexA* is a DNA damage response coordinator that permits two opposite responses: life, mediated by the SOS, and death, mediated by the ALD. The choice seems to be a function of the degree of DNA damage in the cell.**

Received 3 June 2014 **Accepted** 16 June 2014 **Published** 15 July 2014

Citation Erental A, Kalderon Z, Saada A, Smith Y, Engelberg-Kulka H. 2014. Apoptosis-like death, an extreme SOS response in *Escherichia coli*. mBio 5(4):e01426-14. doi:10.1128/mBio.01426-14.

Editor Patricia Rosa, NIAID, NIH

Address correspondence to Hanna Engelberg-Kulka, hanita@cc.huji.ac.il.

This article is a direct contribution from a member of the American Academy of Microbiology.

Programmed cell death (PCD) is an active process resulting in cell suicide. Today, any form of cell death mediated by an intracellular death program, no matter what triggers it, is called PCD (1). All eukaryotes have well-regulated PCD pathways built into their genes, which help sculpt organs during development and scuttle infected cells before they get out of control (1–4). Apoptosis, the classical form of eukaryotic PCD, is specifically characterized by DNA fragmentation and membrane depolarization (5–8).

As in many bacteria, the chromosome of *Escherichia coli* bears the toxin-antitoxin module *mazEF* (9). In *E. coli*, *mazEF* is responsible for nonapoptotic bacterial PCD (10). The *mazF* gene specifies the stable toxin MazF, and the *mazE* gene specifies the labile antitoxin MazE, which is degraded by the ClpPA protease (9). Various stressful conditions, including damage to the DNA, induce *E. coli* MazF (11–13), a sequence-specific endoribonuclease cleaving at ACA sites in mRNAs (14). Furthermore, the induction of MazF leads to the generation of a unique alternative translation machinery composed of leaderless mRNA and ribosomes in which the 16S rRNAs are missing their last 43 nucleotides (15). This alternative translation machinery is responsible for the selective synthesis of specific proteins, some of which, like YfiD, SlyD, ClpX, and YgcR, are involved in cell death (16).

Recently, we showed that when the *mazEF*-mediated cell death pathway is triggered by severe DNA damage, the operation of an additional cell death pathway in *E. coli* is prevented (10). This second death pathway is mediated by *recA-lexA* and, like *mazEF*, is also triggered by severe DNA damage. However, unlike *mazEF*-mediated cell death, it is characterized by membrane depolarization and DNA fragmentation, two hallmarks of apoptosis (5–8). Therefore, we called this *E. coli* novel death pathway apoptosis-like death (ALD) (10).

A well-known cellular response to DNA damage that is mediated by *recA-lexA* is the extensively studied SOS system (reviewed in references 17 to 21). In an uninduced cell, the *lexA* gene product, LexA, acts as a repressor of more than 40 genes (22, 23), including *recA* and *lexA*, by binding to operator sequences (called an SOS box) upstream from each gene or operon. Damage to the DNA creates regions of single-stranded DNA; single-stranded DNA promotes the conversion of RecA to an active form that can

facilitate the otherwise latent capacity of LexA (and some other proteins like UmuD and the λCI repressor) to autodigest (18, 20–22, 24).

Here, we show that the *E. coli mazEF* pathway inhibits not only the ALD pathway but also the SOS response. In addition, we have more fully characterized ALD and the differences between the SOS response and ALD. Accordingly, ALD, unlike SOS, occurs only under severe DNA damage, and it has the following additional characteristics of apoptosis: (i) rRNA degradation by the endoribonuclease YbeY, (ii) upregulation of a unique set of genes that we called extensive-damage-induced (*Edin*) genes, (iii) a decrease in the activities of complexes I and II of the electron transport chain, and (iv) the formation of high levels of $OH^{\cdot}$ through the Fenton reaction, eventually resulting in cell death. Thus, our results revealed that LexA-RecA is a DNA damage response coordinator that permits two opposite responses: life, mediated by SOS, and death, mediated by ALD. We found that the mechanism for choosing between life and death is related to the concentration of the DNA-damaging agent that we used to treat the cells. Thus, the choice seems to be a function of the degree of DNA damage in the cell.

RESULTS

The SOS response is inhibited by the *mazEF* pathway. Previously, we reported that the *mazEF* pathway inhibits the *recA-lexA*-dependent ALD pathway (10). Since the SOS response is known to be *recA-lexA* dependent, we asked whether the *E. coli mazEF* pathway also inhibits the SOS response. To study the SOS response, we used plasmid pL(*lexO*)-*gfp* (25), which bears *gfp*, the gene for green fluorescent protein (GFP), under the control of the *lexA* operator, *lexO*. In this system, under uninduced conditions, LexA represses *gfp* transcription by binding to the SOS box in the gene operator, *lexO*. Under the stressful condition of DNA damage, RecA becomes activated and acts as a coprotease that stimulates the inactivation of LexA by autocleavage (18), allowing the *gfp* gene to be transcribed and its fluorescence to be detected. Thus, in this system, fluorescence is a reporter for the RecA-dependent SOS response. Using this fluorescence reporter system, we caused moderate DNA damage by adding 10 μg/ml nalidixic acid (NA) to the cultures. We observed no fluorescence in the wild-type (WT) strain; we did observe fluorescence in the strain lacking *mazEF* (Fig. 1A). Thus, the SOS response did not take place in the *E. coli* WT strain MC4100*relA*$^+$ but only in strain MC4100*relA*$^+$Δ*mazEF*, from which the *mazEF* genes had been deleted (Fig. 1A). Note that the SOS response can be observed after treatment with 10 μg/ml NA. We found similar results when we caused DNA damage by adding norfloxacin (see Fig. S1A in the supplemental material) or by treatment with UV irradiation (see Fig. S1B). Our results suggest that the SOS response cannot take place in the presence of *mazEF*.

Previously, we found that the nutritional starvation signal (p)ppGpp, responsible for the stringent response (26), is involved in the *mazEF*-mediated cell death (9). Here, we asked whether the SOS response was permitted in *E. coli* strains defective in (p)ppGpp production. To this end, we first used *E. coli* strain MC4100relA1 in which the *relA* gene is impaired by an insertion (*relA1*) (27). Indeed, we did observe the SOS response in the MC4100*relA1* strain (see Fig. S2 in the supplemental material). This result explains the reason for the induction of the SOS response in MC4100*relA1*, although this strain carries a *mazEF* module (26).

Previously, we also reported that the induction of the *mazEF*-mediated death pathway activates the selective synthesis of two groups of proteins: the products of genes *yfbU*, *slyD*, *yfiD*, *clpP*, and *ygcR*, which participate in the death process (the "death genes"), and the products of genes *elaC* and *deoC*, which lead to cell survival (the "survival genes") (16). Here, we found that the SOS response took place in cells from which we deleted any one of the individual death genes (Fig. 1B to F); however, as in the WT strain, the SOS response did not take place in cells from which we deleted either of the survival genes *deoC* and *elaC* (Fig. 1G and H). These results suggest that the SOS response requires the absence of either *mazEF* or one of the other death genes.

In addition to the use of plasmid pL(*lexO*)-*gfp*, we also studied SOS by following the increase in mRNA levels of *dinB* and *umuC*, which are known to be induced as part of the SOS response (21). As in the case of pL(*lexO*)-*gfp*, under the condition of SOS induction with 10 μg/ml NA, the levels of both *dinB* and *umuC* are not increased in the WT strain MC4100*relA*$^+$, but they are significantly elevated in its Δ*mazEF* derivative (see Fig. S3 in the supplemental material).

ALD-mediated DNA fragmentation occurs only under conditions of severe DNA damage. Previously, we showed that one of the characteristics of *E. coli* ALD is membrane depolarization, a hallmark of eukaryotic apoptosis. This membrane depolarization takes place only under conditions of severe DNA damage (above 50 μg/ml NA) (10). We wondered if DNA fragmentation, the other characteristic common to both eukaryotic apoptosis and *E. coli* ALD, might also occur only under conditions of severe DNA damage. To this aim, we treated *E. coli* strain MC4100relA$^+$ (WT) and its Δ*mazEF* derivative with either a low (10-μg/ml) or a high (100-μg/ml) concentration of NA. We found that DNA fragmentation occurred only in the absence of *mazEF* (in strain MC4100*relA*$^+$Δ*mazEF*) and only when the strain was exposed to a high concentration of NA (100 μg/ml) (Fig. 2E), not a low concentration of NA (10 μg/ml) (Fig. 2F). Thus, with a low concentration of NA, which we have shown to induce the SOS response (Fig. 1), DNA fragmentation does not take place. Thereby, we could distinguish the SOS response from ALD as a function of the concentration of the agent causing the DNA damage.

rRNA degradation is an additional characteristic of ALD. In metazoans, apoptosis involves not only irreversible DNA damage but also cleavage in specific places on several RNA species, including 28S rRNA, U1 snRNA, and Ro RNP-associated Y RNAs (28). In addition, when the yeast *Saccharomyces cerevisiae* was exposed to a variety of stimuli known to induce apoptosis, the two rRNAs 25S and 5.8S were degraded extensively (29). Here, we asked whether RNA degradation is involved in *E. coli* ALD. As in our previous experiments, we treated the WT *E. coli* strain MC4100relA$^+$ and its Δ*mazEF* derivative with 100 μg/ml NA. Then, we extracted the RNA and determined the integrity of the RNA. We found that massive degradation of the 16S and 23S rRNAs occurred only in the Δ*mazEF* derivative and only when it was treated with a high concentration (100 μg/ml) of NA, the characteristic conditions for ALD (Fig. 3A). However, the degradation of the rRNAs does not occur under a low concentration of NA (10 μg/ml) (Fig. 3A), which we showed to induce the SOS response (Fig. 1). In addition, after treating the Δ*mazEF* strain with a high concentration (100 μg/ml) of NA, we followed the

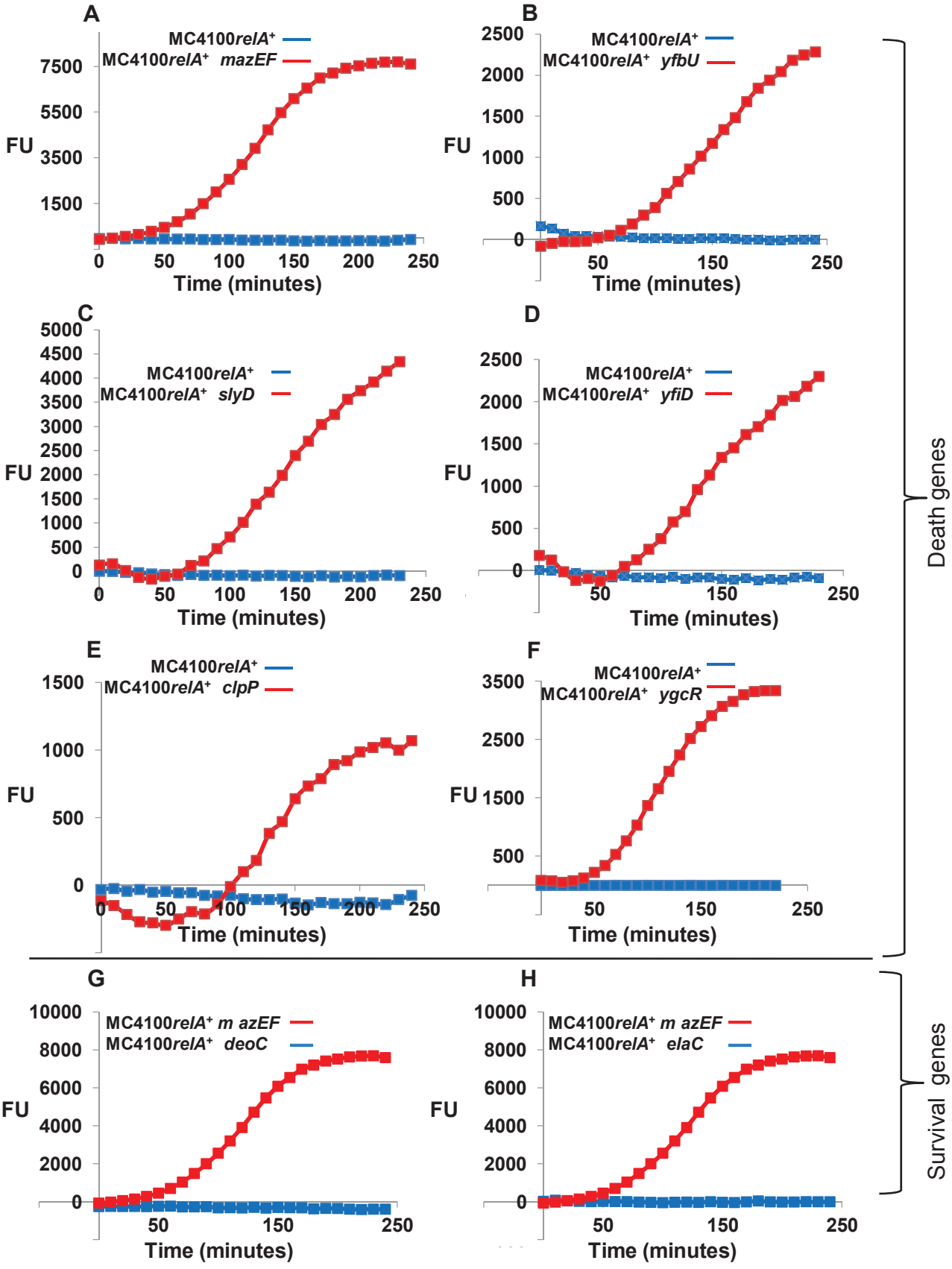

FIG 1 Effects of the *mazEF* module, and genes downstream from *mazEF*, on the SOS response. For the effect of the death genes, we compared *E. coli* WT strain

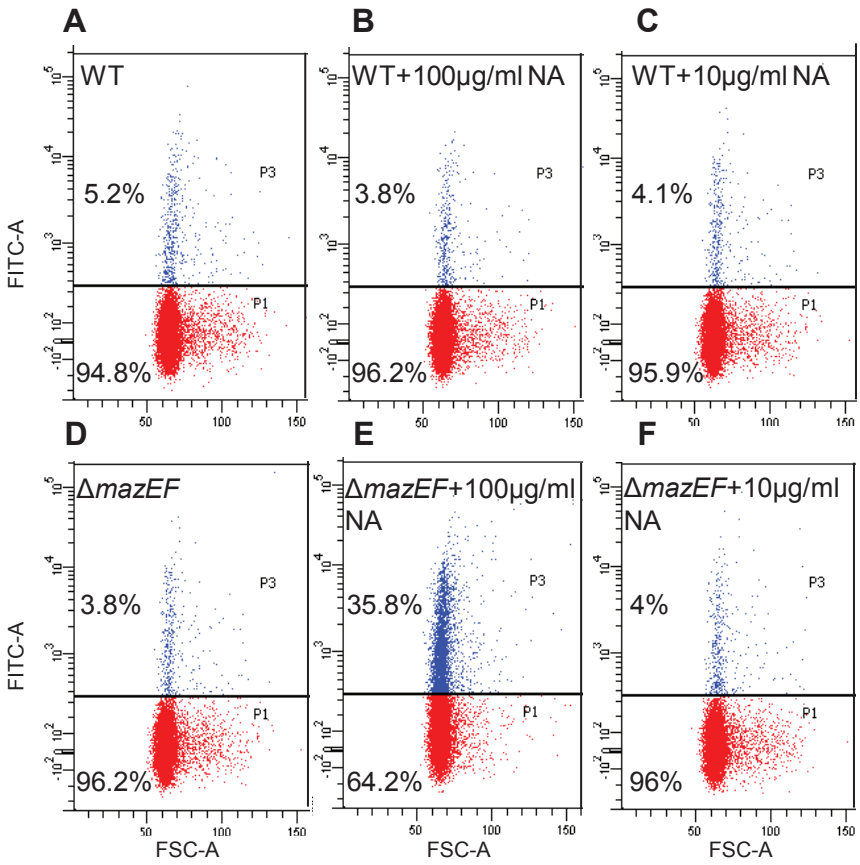

FIG 2 DNA fragmentation as a function of treatment with three concentrations of nalidixic acid (detected by TUNEL assay). WT *E. coli* MC4100*relA*$^+$ (A to C) or MC4100*relA*$^+$Δ*mazEF* (D to F) was grown to an OD_{600} of 0.6. Each culture was divided into three samples that were treated with the addition of no NA, 100 μg/ml NA, or 10 μg/ml NA. DNA fragmentation was determined using the Apo-Direct kit (10). The location of the horizontal threshold line between TUNEL-negative cells (highlighted in red) and TUNEL-positive cells (highlighted in blue) was determined using untreated, unstained MC4100*relA*$^+$ cells. These data represent the results of one of three similar experiments. FITC, fluorescein isothiocyanate; FSC, forward scatter.

progress of 16S rRNA and 23S rRNA degradation over time (Fig. 3B). After half an hour, we observed some degradation of the 23S rRNA; this degradation continued gradually over 4 h, at the end of which time we found that most of the 23S rRNA was completely degraded. The degradation of the 16S rRNA started later, only after 1.5 h of treatment, and by 4 h, most of the 16S rRNA was degraded (Fig. 3B).

We asked which enzyme is responsible for the degradation of the rRNA under conditions permitting ALD. Recently, Jacob and colleagues (30) showed that YbeY, a previously unidentified endoribonuclease, and the exonuclease RNase R (encoded by *rnr*) act together to degrade defective 70S ribosomes, sparing properly matured 70S ribosomes and intact individual subunits. Here, from strain MC4100*relA*Δ*mazEF*, we deleted each of these RNases separately. Deleting the *rnr* gene did not affect RNA degradation (Fig. 3C). However, deleting the *ybeY* gene clearly prevented the degradation of the 23S rRNA, and instead of the 16S rRNA, we found two other products: one of them seems to be a 17S rRNA and the second is smaller than the 16S rRNA (Fig. 3C). Since Jacob and colleagues (30) showed that YbeY is involved in the critically important processing of the 3′ terminus of the 16S rRNA, we think that this 17S rRNA might be a precursor of the 16S rRNA. We do not have yet a clue to the nature of the other product, which is smaller than the 16S rRNA. Our results show that, under conditions leading to ALD, the product of the *ybeY* gene, but not that of the *rnr* gene, was involved in the degradation of rRNA. Thus, we have shown that ALD was characterized not only by membrane depolarization and DNA fragmentation (10) but also by rRNA degradation. Moreover, like the other properties of ALD, RNA degradation occurred only when cells were treated with a high concentration of NA. Based on these results, we suggest that treatment with a high concentration of NA is the condition for ALD; treatment with a low concentration of NA is the condition for SOS.

Figure Legend Continued

MC4100*relA*$^+$ and its Δ*mazEF* (A), Δ*yfbU* (B), Δ*slyD* (C), Δ*yfiD* (D), Δ*clpP* (E), and Δ*ygcR* derivatives (F). For the effect of the survival genes, we compared the WT Δ*deoC* (G) and Δ*elaC* (H) (marked in blue) derivatives with MC4100*relA*Δ*mazEF*. All of these strains harbored plasmid pL(lexO)-*gfp*. After growing the cells in M9 medium with added ampicillin (100 μg/ml) and with shaking at 37°C to an OD_{600} of 0.5 to 0.6, we treated (time zero) them (or not) with 10 μg/ml NA. We measured fluorescence units (FU) using a fluorometer over a period of 4 h (240 min). All of the values shown are relative to those of the control cells not treated with NA.

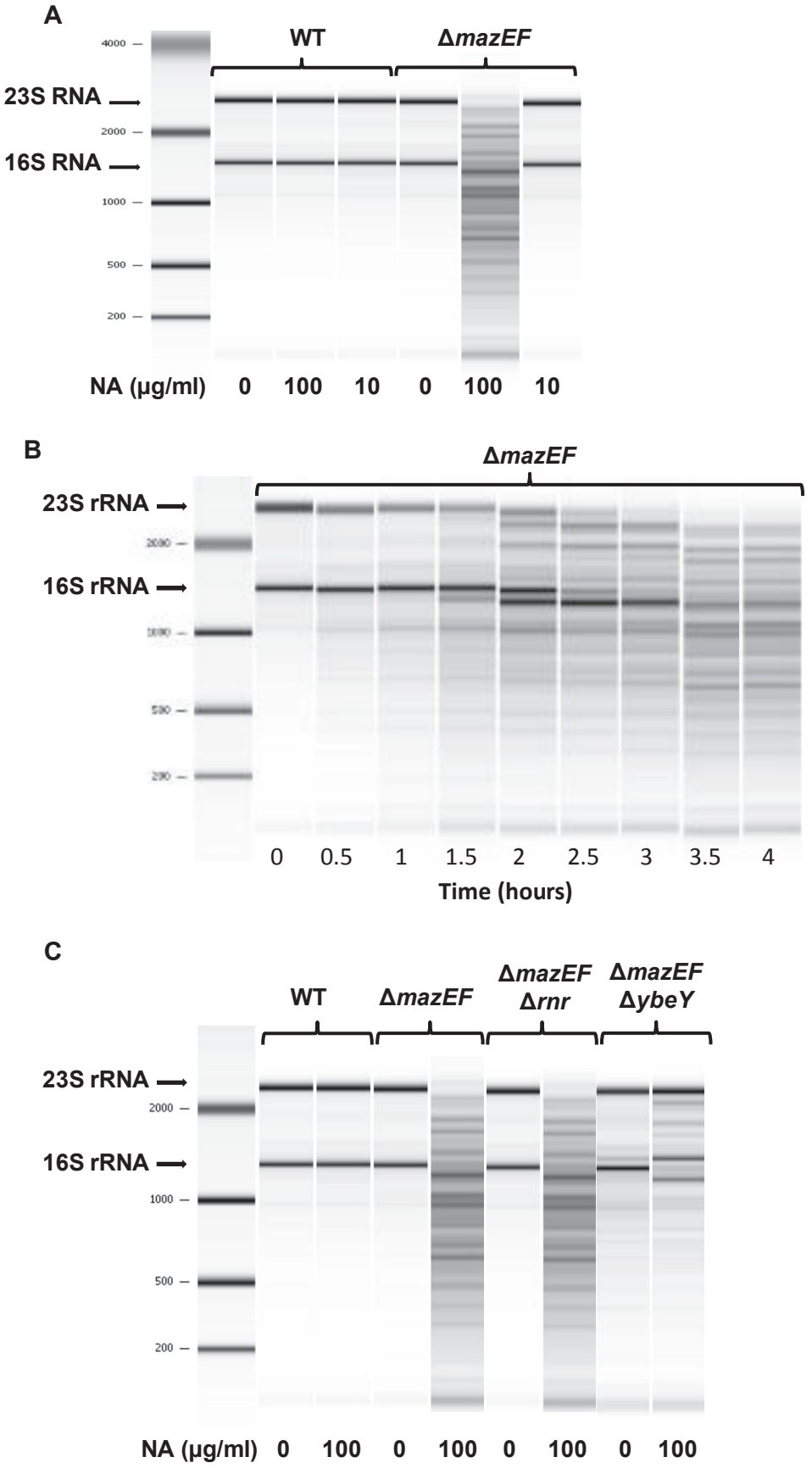
A
WT
ΔmazEF
4000
23S RNA
2000
16S RNA
1000
500
200
NA (μg/ml) 0 100 10 0 100 10
B
ΔmazEF
23S rRNA
16S rRNA
0 0.5 1 1.5 2 2.5 3 3.5 4
Time (hours)
C
WT
ΔmazEF
ΔmazEF Δrnr
ΔmazEF ΔybeY
23S rRNA
2000
16S rRNA
1000
500
200
NA (μg/ml) 0 100 0 100 0 100 0 100

Viability assays distinguish between ALD and SOS. To further distinguish between ALD and the SOS response, we measured the cell survival (CFU) of *E. coli* WT strain MC4100*relA*$^+$ and its Δ*mazEF* derivative under the condition of extensive DNA damage (100 μg/ml NA) and under the condition of moderate DNA damage (10 μg/ml NA). When we applied 100 μg/ml NA, the *mazEF* death pathway in the WT strain caused a reduction in cell survival of about 5 orders of magnitude. Under the same condition, in the strain lacking *mazEF* (Δ*mazEF*), the ALD pathway caused a reduction in cell survival of about 4 orders of magnitude (see Fig. S4A in the supplemental material). In contrast, when we applied 10 μg/ml NA, we observed a reduction in viability of about 3 orders of magnitude only in the WT strain in which the *mazEF* death pathway was functioning; under this condition, cell survival was only slightly affected in the Δ*mazEF* strain (Fig. S4B), suggesting that ALD was not functioning. It seems likely that the killing effect was spared by the SOS response, which we have found to be induced under such conditions (Fig. 1A). In summary, our results suggest that in the absence of the *mazEF* pathway (Δ*mazEF*), the cellular response depends on the intensity of the DNA damage: moderate DNA damage led to the SOS response and cell survival (Fig. S4B), and severe DNA damage activated the ALD pathway, leading to cell death (Fig. S4A). Thus, we found previously that ALD leads to membrane depolarization and DNA fragmentation (10), and we found here that ALD led also to RNA degradation (Fig. 3) and eventually to cell death (Fig. S4A).

LexA degradation is increased under the conditions of ALD. Previously, we showed that, like the better-known SOS response, ALD is *recA*-*lexA* dependent (10). Here, we hypothesize that we can distinguish between the ALD response and the SOS response by the degree of RecA coprotease activity. We determined RecA coprotease activity by measuring LexA degradation. After various time periods, under conditions of ALD (100 μg/ml NA) or SOS (10 μg/ml NA), we extracted proteins from the WT strain and its Δ*mazEF* derivative. We quantified LexA degradation by subjecting the proteins to Western blot analysis using anti-LexA antibody. As *lexA3* encodes a noncleavable LexA repressor (31), as a control we used a *lexA3* mutant of *E. coli* strain MC4100relA$^+$Δ*mazEF* (10). As expected, under all conditions tested, LexA was not degraded in either the WT or the *lexA3* mutant: the LexA protein remained intact (Fig. 4). In contrast, in the Δ*mazEF* strain, LexA was partially degraded under the SOS conditions (10 μg/ml NA) and totally degraded under the ALD conditions (100 μg/ml NA) (Fig. 4). This degradation was visible within 1 h of incubation with 100 μg/ml NA. LexA degradation also took place in MC4100*relA*$^+$ mutants from which we deleted not *mazEF* itself but rather the gene *yfiD* or *slyD* downstream *of mazEF* (Fig. 4). Here also, LexA degradation can be observed mainly under the ALD conditions (100 μg/ml). However, in this experiment, it can minimally be observed under the SOS conditions (10 μg/ml). Altogether, we see that (i) in the WT strain, in the presence of the *mazEF* system, RecA is not active as a coprotease, and (ii) in the absence of the *mazEF* system, RecA is more active as a coprotease under ALD conditions (treatment with 100 μg/ml NA) than under the condition of the SOS response (treatment with 10 μg/ml NA).

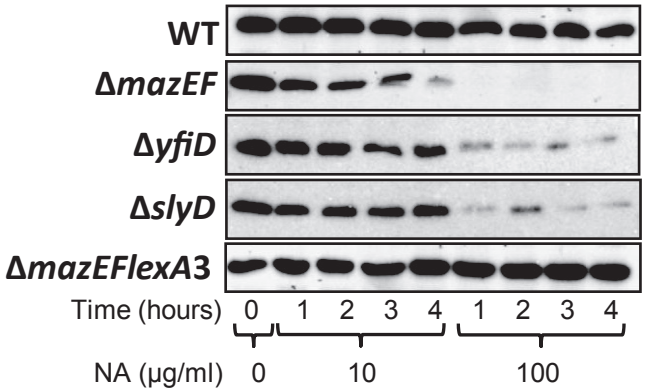

FIG 4 LexA degradation is increased under high concentrations of nalidixic acid in the absence of the *mazEF* pathway. The degree of LexA degradation was reflected by the level of RecA activity. WT *E. coli* strain MC4100relA$^+$ and each of its Δ*mazEF*, Δ*yfiD*, Δ*slyD*, and Δ*mazEFlexA3* derivatives were grown to an OD_{600} of 0.5. Each culture was divided into three aliquots to which appropriate concentrations of nalidixic acid (NA) were added. These samples were incubated for up to 4 h. At the times indicated, cells were lysed and the proteins were analyzed by Western blot analysis using rabbit polyclonal antibody to the LexA DNA binding region.

The ALD pathway includes the expression of a new set of genes of the *E. coli* oxidative respiratory system. Having found that LexA degradation was significantly higher under ALD than under SOS conditions, we hypothesized that additional genes tightly regulated by LexA would be transcribed under ALD conditions. We used microarray analysis to test the transcription pattern of upregulated genes in ALD. We added no NA (no treatment [n.t.]), 100 μg/ml NA, or 10 μg/ml NA to cultures of the WT strain MC4100*relA*$^+$ or its Δ*mazEF* or Δ*mazEFlexA3* derivatives. We extracted the RNA and compared the gene expression of treated samples with that of the untreated sample, resulting in 6 lists of upregulated genes (see Fig. S5A in the supplemental material, lists 1 to 6). We wished to focus on the ALD pathway genes that were specifically upregulated only in the Δ*mazEF* derivative and only after treatment with 100 μg/ml NA. To separate the nonspecifically upregulated genes (Fig. S5A, list 1, and Fig. S5B, blue oval area marked "1") from the specifically upregulated genes (Δ*mazEF* + 100 μg/ml NA), we eliminated all of the expressed genes that had been induced in the other 5 lists (Fig. S5B and C), resulting in a list of 190 specifically upregulated genes (Fig. S5A, bottom row). We saved only one copy of genes that appeared no more than once, leaving 162 genes of the ALD pathway (see Table S1). After eliminating 42 of these genes whose functions are not yet known, we divided the remaining 120 genes by function (Fig. S5D and Table S1). In addition to the 8 known SOS genes, we

FIG 3 *E. coli* ALD is also characterized by rRNA degradation. (A) rRNA degradation occurs only at high NA concentrations and only in the Δ*mazEF* strain. *E. coli* MC4100*relA*$^+$ (WT) or its Δ*mazEF* derivative was grown to an OD_{600} of 0.5. Each culture was divided into three samples that were treated with the addition of 100 μg/ml NA or 10 μg/ml NA or not treated. To detect RNA degradation, after 4 h of incubation without shaking at 37°C, RNA was extracted and a Bioanalyzer was used to determine the integrity of the RNA. (B) rRNA degradation in Δ*mazEF* cells over time. MC4100*relA*$^+$Δ*mazEF* was grown, treated, and incubated with 100 μg/ml NA as in panel A. At the times indicated, RNA integrity was determined as described for panel A. (C) The *ybeY* gene but not the *rnr* gene is involved in the degradation of rRNA in the *E. coli* Δ*mazEF* derivative. WT MC4100*relA*$^+$ and its Δ*mazEF*, Δ*mazEF*Δ*rnr*, or Δ*mazEF*Δ*ybeY* derivative were grown and treated with 100 μg/ml NA as described for panel A. RNA was extracted, and its integrity was determined as described for panel A.

were amazed to find 5 tricarboxylic acid (TCA) cycle genes, 7 respiratory electron transport chain genes, and 12 Fe-S cluster genes, all of which were specifically upregulated.

Under ALD conditions, the activities of respiratory electron transport chain complexes I and II are decreased. In our microarray results, the genes upregulated only under ALD conditions included genes of the electron transport chain system, suggesting that ALD conditions may affect the activity of that system. The upregulated genes included *nuoG*, *sdhA*, and *sdhB*. *nuoG* encodes NADH dehydrogenase I (NuoG), which transfers electrons from NADH to respiratory system complex I. SdhA and SdhB, products of *sdhA* and *sdhB*, are two subunits of succinate dehydrogenase (SDH), which transfers electrons in the electron transfer chain from succinate to flavin adenine dinucleotide (FAD) in complex II. We tested NADH dehydrogenase I (complex I) and succinate dehydrogenase (complex II) activities. Since the microarray analysis revealed upregulation of genes in the respiratory chain, we expected increases in the activities of both complexes I and II. Instead, under ALD conditions (4 h with 100 μg/ml NA), although complex II activity increased in the WT strain, it drastically decreased (about 90%) in the Δ*mazEF* strain (Fig. 5B). Under the same conditions, the activity of complex I decreased significantly more in the Δ*mazEF* strain (about 56%) than in the WT strain (about 28%) (Fig. 5A). Note that under SOS conditions (4 h with 10 μg/ml NA), complex II activity increased in both the WT and its Δ*mazEF* derivative (see Fig. S6B in the supplemental material). In strain MC4100*relA*$^+$*lexA3*Δ*mazEF*, in which the LexA repressor is not cleaved, under ALD conditions, the activities of complexes I and II did not decrease (Fig. 5A and B), indicating that the decreases were *recA-lexA* dependent. Under ALD conditions, these decreases in activity might be dependent on 9 Fe-S clusters in complex I and 4 Fe-S clusters in complex II. This possibility is supported by our measurements of the activity of *E. coli* NADH dehydrogenase II (Fig. S6C), which, instead of Fe-S clusters, contains a thiol-bound Cu(I) and a putative copper binding site (32). Under ALD conditions, we observed no change in NADH dehydrogenase II activity (Fig. S6C). Our combined results suggest that, under ALD conditions, mainly complex II activity was decreased.

ALD conditions induce high levels of OH• formation. In eukaryotic cells, mitochondrial membrane depolarization causes reactive oxygen species (ROS) production, important for inducing apoptosis (33). In mitochondrial apoptosis, NDUFS1 protein from complex I (an NADH dehydrogenase of the electron transport chain) is cleaved by caspases, leading to the production of ROS (34). Under ALD conditions, we observed decreased activity in the electron transport chain (especially in complex II activity) (Fig. 5; see also Fig. S6 in the supplemental material), so we asked whether in *E. coli*, in the absence of *mazEF*, ROS would be formed under the ALD conditions. The hydroxyl radical ($OH^{\cdot}$), which is highly hazardous to the cell, is the final product of the Fenton reaction. We examined OH production under ALD conditions. We grew cells and treated them with NA (100 μg/ml). We measured the formation of OH using hydroxyphenyl fluorescein (HPF), which is nonfluorescent until it reacts with OH. While we detected no OH formation in the WT strain (Fig. 6A), we detected relatively high levels of OH formation in the Δ*mazEF* strain (Fig. 6B). Under the ALD condition, we also detected $OH^{\cdot}$ formation (see Fig. S7A and B), as well as membrane depolarization (see Fig. S7C and D), in strain MC4100*relA1*, which carries WT *mazEF* but an impaired *relA* (27). As was shown by us above, this strain permits also the SOS response (Fig. S2), probably because the function of *mazEF* is prevented due to impairment in the production of (p)ppGpp. In addition, the $OH^{\cdot}$ levels in strain MC4100*relA*$^+$Δ*mazEF* were higher under ALD conditions (100 μg/ml NA) than under SOS conditions (10 μg/ml NA) (Fig. 6B). $OH^{\cdot}$ formation could also be detected in the derivatives deleted in *yfiD* or *slyD* (acting downstream of the *mazEF* gene) but only under ALD conditions (100 μg/ml NA) (see Fig. S8A and B). We also asked if $OH^{\cdot}$-neutralizing agents would prevent ALD. To neutralize $OH^{\cdot}$, we used thiourea (an $OH^{\cdot}$ scavenger) or dipyridyl (a Fe_2^+ chelator and thereby an inhibitor of the Fenton reaction). We studied four ALD hallmarks: membrane depolarization, RNA degradation, LexA degradation, and reduction in viability. The addition of either thiourea or dipyridyl prevented membrane depolarization (Fig. 6C) and RNA degradation (Fig. 6D) and reduced RecA coprotease activity (reflected by LexA cleavage [see Fig. S9A in the supplemental material]). Furthermore, adding dipyridyl or thiourea to the growth medium reduced cell killing by NA (100 μg/ml) by about 2 orders of magnitude (see Fig. S9B). Note that adding either thiourea or dipyridyl also prevented HPF staining, supporting the notion that the HPF staining is specific to $OH^{\cdot}$ formation (see Fig. S9C).

Gene *iscS* codes for ISC cysteine desulfurase, responsible for Fe-S cluster formation; deleting *iscS* abolishes the Fenton reaction (35). Since our results suggest that the Fenton reaction is involved in ALD, we wished to clarify the involvement of *iscS* under ALD conditions. Indeed, deleting *iscS* from the Δ*mazEF* strain prevented $OH^{\cdot}$ formation (compare Fig. 6E and F) and membrane depolarization (compare Fig. 6G and H), making the formation of high levels of $OH^{\cdot}$ another hallmark of ALD and probably the cause of its lethal effect on *E. coli*. Note that under SOS conditions the levels of $OH^{\cdot}$ in the Δ*mazEF* derivative were much lower than those under ALD conditions (Fig. 6B).

DISCUSSION

Though both are mediated by RecA-LexA, *E. coli* ALD and SOS appear to be two different responses. In the 1970s, Radman first described the bacterial response to DNA damage, calling it the "SOS response" (19). So far, it is the largest, most complex, and best-understood bacterial DNA damage-inducible network (17–21, 24). In the SOS regulatory network, gene expression is controlled by a complex circuit involving RecA and LexA (21). Inducing SOS leads to the generation of regions of single-stranded DNA. In the presence of nucleotide triphosphates, when RecA binds to these regions of single-stranded DNA a nucleotide filament is generated that converts RecA to an active form. Activated RecA facilitates the otherwise latent capacity of LexA (and additional proteins) to undergo self-cleavage (18, 20–22, 24).

Previously, we showed that *E. coli* apoptosis-like death (ALD) is also mediated by *recA-lexA*. We showed that ALD shared two hallmarks with eukaryotic mitochondrial apoptosis: membrane depolarization and DNA fragmentation. Based on our previous work showing that membrane depolarization occurs only under a high concentration of NA (above 50 μg/ml), we suggested that ALD is an SOS response to extreme DNA damage (10).

Here, we found that ALD shares additional hallmarks with eukaryotic mitochondrial apoptosis, including rRNA degradation (Fig. 3) and the formation of high levels of $OH^{\cdot}$ (Fig. 6). Moreover, we found that ALD is also characterized by the induction of the

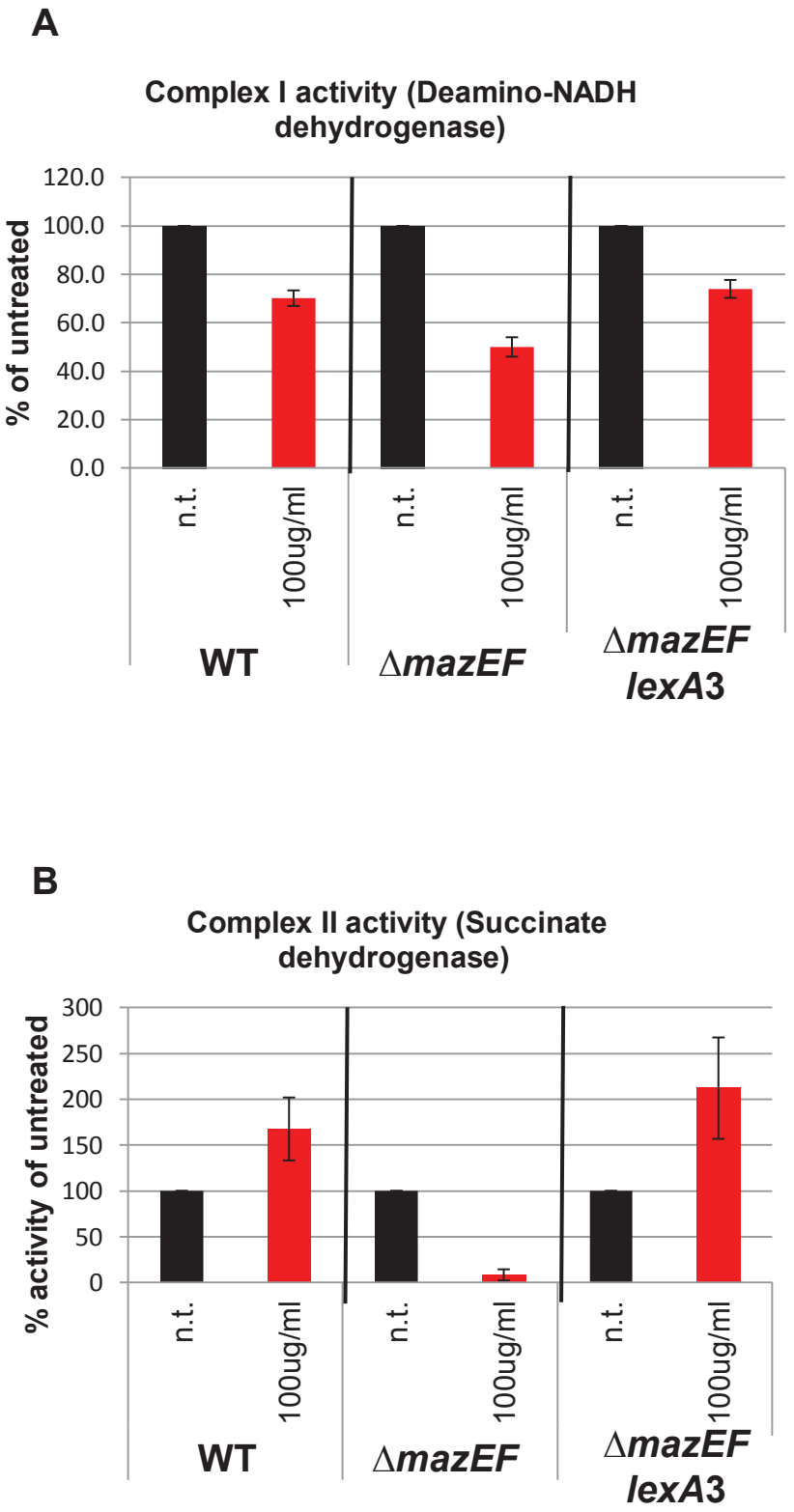

FIG 5 Complex I and complex II activities are decreased by high concentrations of NA in the Δ*mazEF* derivative of MC4100*relA*$^+$. *E. coli* strains MC4100*relA*$^+$, MC4100*relA*$^+$Δ*mazEF*, and MC4100*relA*$^+$*lexA*3Δ*mazEF* were grown to an OD_{600} of 0.5. Each culture was divided into two samples to which either no NA (n.t.) or 100 μg/ml NA was added. After 4 h of incubation, total proteins were extracted. Enzymatic activities were determined as described in Materials and Methods. (A) Complex I activity (NADH dehydrogenase I) was determined by measuring the reduction levels of deamino-NADH. (B) Complex II activity (succinate dehydrogenase) was determined by measuring the reduction levels of dichlorophenol indophenol. These data represent the results of three experiments.

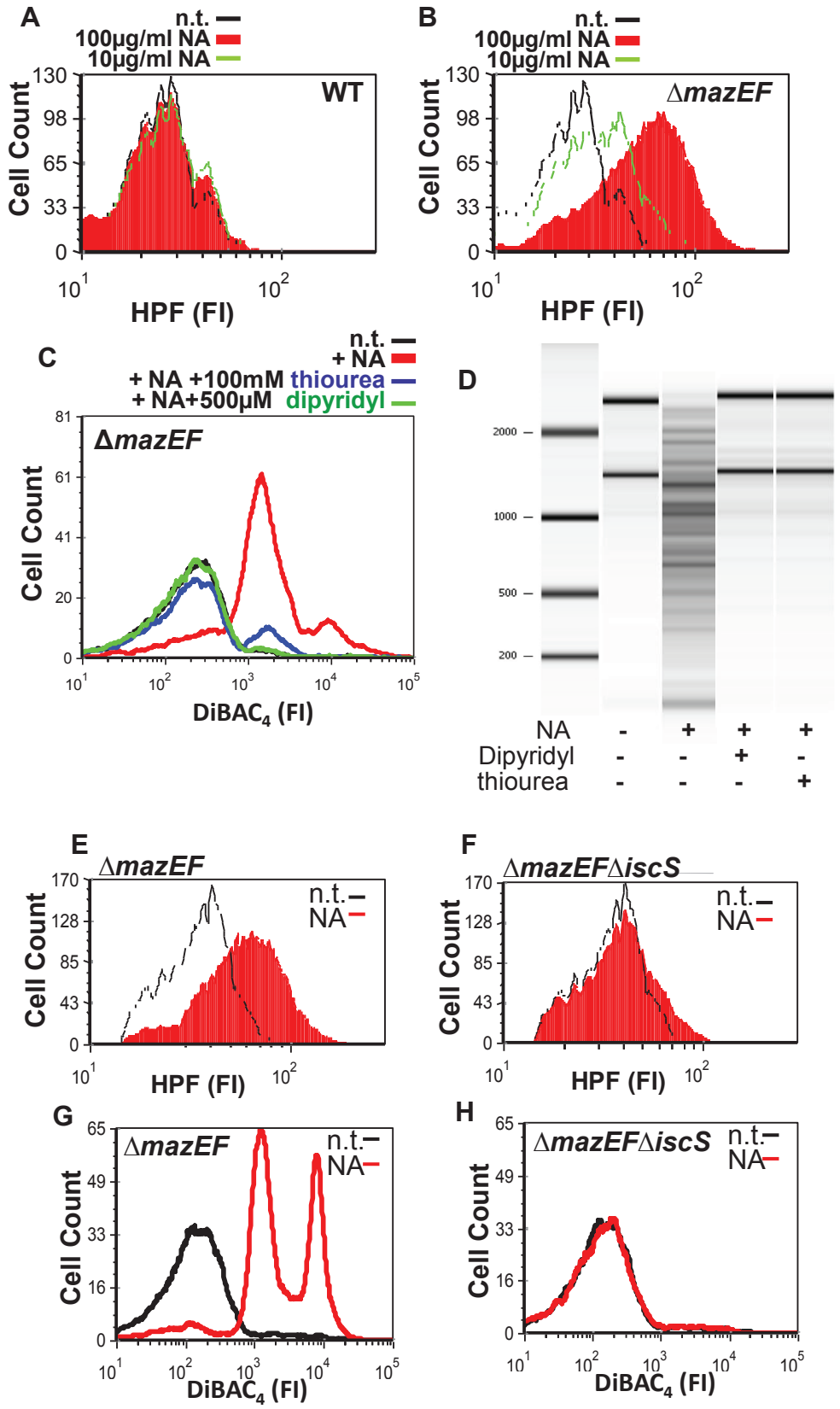

FIG 6 ALD involves high levels of OH· formation and is prevented by Fe_2^+ chelator and by the *mazEF* pathway. (A and B) OH· formation was determined by HPF staining. *E. coli* WT strain MC4100*relA*$^+$ (A) or its Δ*mazEF* derivative (B) was grown to an OD_{600} of 0.5. Each culture was divided into three samples that were treated with the addition of 100 µg/ml NA or 10 µg/ml NA or not treated. After 4 h of incubation, the cells were stained with HPF to detect the formation

(Continued)

expression of a new set of genes that we called extensive-damage-induced (*Edin*) genes (see Fig. S5 in the supplemental material). Finally, we found that ALD also involved a decrease in the activities of respiratory system complexes I and II (Fig. 5; see also Fig. S6). All of these ALD hallmarks, including membrane depolarization and DNA fragmentation as we have previously reported (10), are inhibited by the *mazEF* pathway (Fig. 3, 5, and 6). We also found that these ALD hallmarks occurred only when the cells were treated with a high concentration of NA (Fig. 2, 3 4, and 6; see also Fig. S4); treatment with a low concentration of NA induced the SOS response (Fig. 1). Our results support the hypothesis that *E. coli* ALD and SOS are two responses, both mediated by *recA-lexA* but activated under different conditions. ALD is activated when the cell experiences high concentrations of DNA-damaging agents; SOS is activated when the cell experiences low concentrations of DNA-damaging agents. Thus, it seems likely that the degree of the DNA damage is what leads to the choice between SOS and ALD. Our results also revealed that, as in the case of the ALD pathway (10), the SOS response is also inhibited by the *mazEF*-mediated pathway (Fig. 1). In both ALD and the SOS response, in addition to *mazF*, the death genes downstream from *mazF* also contribute in some way to this inhibition (Fig. 1B to F).

A model for the intertwined pathways: ALD, the SOS response, and the *mazEF* death pathway. Our model for the ALD pathway (Fig. 7A) is based on the idea that the level of RecA activation in the cell is a function of the level of damaged DNA. Recall that activated RecA acts as a coprotease that stimulates the inactivation by autocleavage of the LexA repressor molecule (18). Indeed, we found that LexA was degraded more extensively under ALD conditions (high NA concentration) than under SOS conditions (low NA concentration) (Fig. 4). Under ALD conditions, strong RecA activation led to high levels of LexA degradation, leading to the transcription of a new set of genes that we have called *Edin* (see Table S1 in the supplemental material). We hypothesize that *Edin* genes are tightly regulated by LexA and that, under ALD conditions, at least some of them are responsible for the decreases in the activities of complexes I and II of the respiratory electron transport chain (Fig. 5; see also Fig. S6). In fact, using the *lexA3* allele, which encodes an uncleavable LexA repressor, we showed that the decrease in the activities of complexes I and II depends on the ability of RecA to cleave the LexA repressor: in strain MC4100*relA*$^+$Δ*mazEFlexA3*, we observed no decreases in the activities of complexes I and II (Fig. 5), suggesting that one or more of the products of the *Edin* genes, usually repressed by LexA, may be responsible for the decrease in complex I and complex II activities. It is also likely that the profound decrease in complex II activity might have led to the formation of high levels of OH (Fig. 6). Thus, under ALD conditions, we suggest that the formation of OH$^\cdot$ is as follows: when complex II activity is decreased, fewer free electrons are transferred in the respiratory chain, resulting in the formation of superoxides, which damage iron-sulfur clusters, making ferrous iron available for oxidation by the Fenton reaction. Finally, this leads to OH$^\cdot$ formation that causes double-strand breaks (DSBs) in the DNA (Fig. 2E) and, possibly, cell death (see Fig. S4).

That the ALD pathway may require free ferrous ions oxidized through the Fenton reaction was supported by our results showing that neutralizing the ferrous ions with dipyridyl prevented ALD (Fig. 6; see also Fig. S9 in the supplemental material). The *iscS* gene is responsible for Fe-S cluster formation and the Fenton reaction (35). Deleting *iscS* from the Δ*mazEF* strain prevented the formation of OH$^\cdot$ and membrane depolarization (Fig. 6E to H). Since our experiments show that under the ALD condition, OH$^\cdot$ scavengers can overcome LexA cleavage (see Fig. S9A) and membrane depolarization (see Fig. S9C), we suggest that OH$^\cdot$ production is upstream of membrane depolarization (Fig. 7A). It seems also possible that under ALD conditions, in addition to mediating cell death ALD might also amplify RecA activity. Under these conditions, high levels of OH$^\cdot$ formation (Fig. 6B) probably damage the DNA (Fig. 2E) and are causing double-strand breaks (DSBs) (Fig. 7A). These DSBs would eventually result in the formation of single-stranded DNA, which in turn would amplify RecA activity (21). This hypothesis is supported by our results from studying the effect on RecA activity of LexA cleavage, which show that inhibition of OH$^\cdot$ formation with dipyridyl or thiourea decreases RecA activity (see Fig. S9A).

We paid special attention to the *Edin* genes, which were upregulated under ALD conditions. In our model (Fig. 7A), upregulated *Edin* genes may be responsible for the decrease in the activity of the electron transport chain and thus play a part in mediating ALD. Alternatively, rather than being ALD mediators themselves, under ALD conditions, the *Edin* genes may be upregulated in response to cell damage. Recall that the gene *nuoG* encodes NADH dehydrogenase I, part of complex I, and that *sdhA* and *sdhB* encode succinate dehydrogenase, which is part of complex II. The upregulation in the expression of these three genes may represent a cell response either to the decrease in complex I and II activities or, alternately, to damage to the protein molecules of these complexes. Further studies are required to elucidate whether *Edin* products are ALD mediators or are produced as a cell response to ALD damage.

We also created a model for the SOS response (Fig. 7B). In contrast to ALD, we found that the SOS response occurred only under conditions of moderate DNA damage (10 μg/ml NA) (Fig. 1). Under these conditions, RecA is only moderately activated, leading to only partial LexA degradation (Fig. 4). Since all

Figure Legend Continued

of OH$^\cdot$. The fluorescence intensity (FI) of the HPF in the cells was determined by FACS. These data represent the results of one of three similar experiments. (C) Thiourea and dipyridyl prevented membrane depolarization. *E. coli* strain MC4100relA$^+$Δ*mazEF* was grown to an OD_{600} of 0.5. The culture was divided into 4 aliquots. To one (control) aliquot, no additions were made (n.t.); to each of the three other aliquots, we added 100 μg/ml nalidixic acid (NA); to one of these, we added 100 mM thiourea scavenger OH$^\cdot$, and to another, we added 500 μM dipyridyl to chelate Fe_2^+ ions. After 4 h of incubation, the cells were stained with $DiBAC_4$. The intensity of the fluorescence (FI) of $DiBAC_4$ in the cells was determined by FACS as described previously (10). Cells that exhibited a $DiBAC_4$ FI value higher than 10^3 were considered to have undergone membrane depolarization. (D) Thiourea or dipyridyl prevented RNA degradation. *E. coli* strain MC4100relA$^+$Δ*mazEF* was grown to an OD_{600} of 0.5. After 4 h of incubation with drugs (100 μg/ml NA and either 500 μM dipyridyl or 100 mM thiourea), RNA was extracted and RNA integrity was determined as described in the legend to >Fig. 3. (E and F) Deleting the *iscS* gene led to a significant reduction in HPF staining. HPF staining was done as described for panels A and B. (G and H) Deleting the *iscS* gene prevented membrane depolarization. Membrane depolarization was done as described for panel C. These data represent the results of one of three similar experiments.

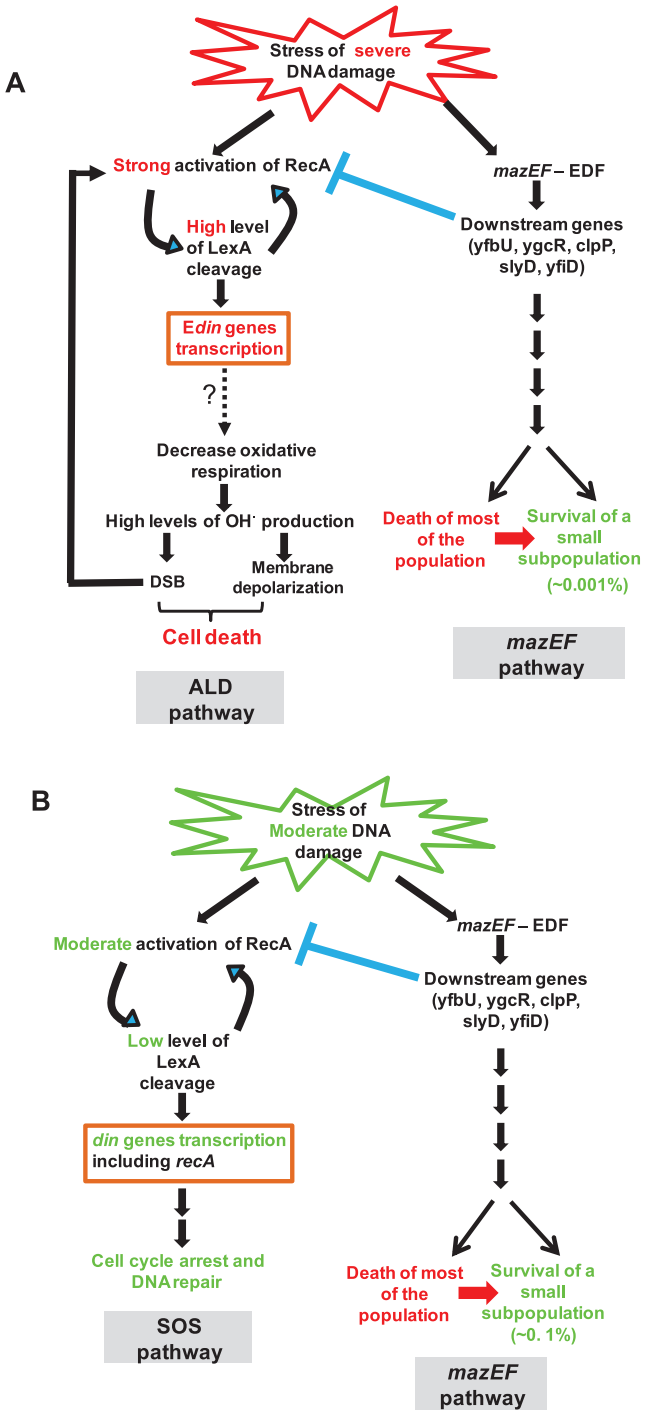

FIG 7 Model for the two *recA-lexA* pathways, ALD (A) and the known SOS response (B), and their inhibition by the EDF-*mazEF* pathway. The EDF-*mazEF*-mediated pathway is activated under both severe (A, right) and moderate (B, right) DNA damage. Under both conditions, we observed a difference only in the level of bacterial survivors (A, right, versus B, right). The EDF-*mazEF*-mediated pathway inhibits the *recA-lexA*-mediated pathway. Therefore, in the absence of a functional EDF-*mazEF*-mediated pathway, the *recA-lexA* pathway is permitted. Under severe DNA damage, strong activation of RecA occurs, leading to the ALD pathway (A, left). On the other hand, under moderate DNA damage, only a moderate activation of RecA occurs, leading to the SOS response (B, left). For additional details regarding the ALD and SOS pathways, see the Discussion. For further details regarding the EDF-*mazEF*-mediated pathway, see references 10, 15, and 16.

din genes are repressed by LexA, partial LexA degradation may permit transcription of these *din* genes, leading to cell cycle arrest and DNA repair activation and, finally, to cell survival (21) (Fig. 7B).

The results of our study suggest that RecA-LexA may be DNA damage response coordinators, permitting one of two opposite responses: life (mediated by the SOS response) (Fig. 7B) and death (mediated by the ALD pathway) (Fig. 7A). The choice between life and death seems to be a function of the degree of DNA damage resulting from the concentration of the DNA-damaging agent to which the cells are exposed (Fig. 2).

Note that both the SOS response and ALD are inhibited by the *mazEF*-mediated pathway (10) (Fig. 1 to 6). This inhibition was not caused directly by MazF activity, since it was also prevented in MC4100*relA*$^+$ derivatives from which we deleted additional genes that act downstream from MazF (10) (Fig. 1, 2, 4, 5, and 6). Until now, we have characterized only 15 out of the 50 genes that act downstream from MazF (16), so we still do not know the exact mechanism of this inhibition. It will be important to elucidate this mechanism, because, as we have suggested previously (10), ALD may be a backup system for the *mazEF*-mediated cell death program. Mutation(s) in one or more of the components of the extracellular death factor (EDF)-*mazEF*-mediated pathway would lead to the formation of EDF-*mazEF* "cheaters," so that the EDF-*mazEF*-mediated pathway would be inactivated. Should that happen, bacterial cell death would occur through the ALD pathway (10).

Evidence for apoptosis-like death in bacteria. Recent research has revealed evidence of apoptotic death in bacteria (summarized in reference 36). Here, we will only specifically describe two of the reports on death induced by DNA damage. Independently of our previous research (10), apoptosis-like death in *E. coli* was also described by Dwyer et al. (37). In addition to membrane depolarization and DNA fragmentation, they found that this apoptosis-like death is also characterized by phosphatidylserine exposure to the outer leaflet of the plasma membrane and chromosome condensation. In particular, they found that RecA can bind peptide sequences that serve as the substrates for eukaryotic caspases, suggesting that RecA acts as a caspase. In contrast to our results showing that ALD is induced only by DNA-damaging agents (10), as they described it (37), apoptosis-like death is induced not only by DNA-damaging agents but also by various antibiotics, including spectinomycin, ampicillin, and gentamicin. Their results (37) may differ from ours (10) because they used LB growth medium while we used M9 and they used *E. coli* strain MG1655 while we used MC4100*relA*$^+$Δ*mazEF*. In earlier work, we showed that MG1655 did not produce the extracellular death factor (EDF) (38) that is required for the enhancement of MazF activity (39) and for the inhibition of ALD (10). Thus, MG1655 behaves like a Δ*mazEF* strain (10). Therefore, it seems to us that, even without deleting the *mazEF* module, Dwyer and colleagues (37) have discovered bacterial apoptosis-like death because the bacterial strain that they used was lacking EDF.

As a whole, our experiments have revealed that the operation of the whole EDF-*mazEF*-mediated pathway is required for the inhibition of ALD. It is possible that, as in *E. coli* strain MG1655, which is deficient in EDF production (38), and MC4100*relA1*, which is impaired in the formation of ppGpp (26), ALD (as well as SOS) will be permitted in some other *E. coli* strains, although they carry the *mazEF* module on their chromosome.

Apoptosis-like death under conditions of DNA damage has also been described in *Caulobacter crescentus* (40), where the executor protein is BapE, which perturbs chromosome integrity by cleaving supercoiled DNA in a sequence-nonspecific manner. The resulting DNA fragmentation, chromosome condensation, and membrane depolarization are characteristic of eukaryotic apoptosis. As far as we know, there is no BapE homologue in *E. coli*.

Evolutionary aspects of bacterial ALD. *E. coli* ALD, having biochemical and morphological hallmarks of apoptosis, may provide additional insight into the evolution of mitochondria and their apoptotic pathway in eukaryotes. It is possible that mitochondria and their apoptotic machinery were evolved during endosymbiosis, when the prokaryotic protomitochondrion was introduced into the primitive protoeukaryotic cell. A relationship between *E. coli* ALD and mitochondria is already indicated in our present study, in which we show that one of the ALD hallmarks is rRNA degradation in which *E. coli* YbeY is involved (Fig. 3). Intriguingly, the mammalian counterpart of YbeY is localized in the mitochondria (41), hinting at a parallel between ALD in *E. coli* and mitochondrial apoptosis. Moreover, YbeY is one of 19 proteins predicted to be involved in complex I disease biology (41). Based on our work here, one might hypothesize that YbeY has a role in eukaryotic mitochondrial apoptosis. Finally, the decrease in complex I and II activities (Fig. 5) led to the formation of high levels of $OH^{\cdot}$ (Fig. 6). *E. coli* complex I activity is carried out by NuoG (NADH dehydrogenase I), which is strikingly similar to the eukaryotic mitochondrial NDUFS1 (42). Cleavage of NDUFS1 by caspases leads to the formation of $OH^{\cdot}$ and eventually to apoptotic death (34).

Further investigation of ALD and other described apoptosis-like pathways (36, 37, 40) may provide more evidence for the origin of mitochondrial apoptosis. One intriguing scenario suggested that eukaryotes developed a control system that would avoid PCD by the endosymbiont machinery. By doing so, in parallel, the ancient eukaryotes made use of them when required (43).

MATERIALS AND METHODS

Bacterial strains and plasmids. We used the following *E. coli* strains: MC4100*relA*$^+$ (WT) (44) and its derivatives MC4100*relA*$^+$Δ*mazEF* (44), MC4100*relA*$^+$Δ*slyD* (16), MC4100*relA*$^+$Δ*yfiD* (16), MC4100*relA*$^+$ *lexA3*Δ*mazEF* (10), and MC4100*relA1* (27). Using the method of Datsenko and Wanner (45), we also constructed *E. coli* strains MC4100*relA*$^+$Δ*mazEF*Δ*rnr*, MC4100*relA*$^+$Δ*mazEF*Δ*ybeY*, and MC4100*relA*$^+$Δ*mazEF*Δ*iscS*. We also used plasmid pL(*lexO*)-*gfp* (25).

Materials and media. Bacterial cultures were grown in liquid M9 minimal medium containing 1% glucose and a mixture of 100 μg/ml of each amino acid except tyrosine and cysteine (38). Nalidixic acid (NA), norfloxacin, thiourea, and 2,2′-dipyridyl were obtained from Sigma (St. Louis, MO, USA). Bis-1,3-dibutylbarbituric acid trimethine oxonol ($DiBAC_4$) and hydroxyphenyl fluorescein (HPF) were purchased from Invitrogen (Carlsbad, CA, USA). To detect DNA fragmentation, we used the Apo-Direct kit purchased from Calbiochem (San Diego, CA, USA).

Growth conditions and viability. For the experiments on membrane depolarization, DNA fragmentation, RNA degradation, microarray analysis, $OH^{\cdot}$ detection, and cell viability, we grew cells in 10 ml M9 minimal medium to an optical density at 600 nm (OD_{600}) of 0.5 to 0.6. Then, we divided each culture into 500-μl aliquots to which we added the appropriate concentration of NA. We incubated each aliquot at 37°C for 4 h (or as described in the figure legends) and then washed them twice with phosphate-buffered saline (PBS) (pH 7.2). We carried out viability assays on LB plates as we have described previously (16). When we used thiourea or 2,2′-dipyridyl, cells were grown as described above and then incubated with 2,2′-dipyridyl (500 μM) or thiourea (100 mM) at 37°C for 10 min. NA was added as described in the figure legends.

Using a GFP reporter to measure the SOS response. To *E. coli* cultures harboring plasmid pL(*lexO*)-*gfp* grown and treated as described above, we added 100 μg/ml ampicillin. Using a 485- ± 15-nm excitation filter and a 530- ± 15-nm emission filter, we measured the fluorescence 25 times in each well at intervals of 10 min. The fluorophore was excited with 1,000-cW lamp energy, and the fluorescence in each well was measured for 1 s (FLUOstar Galaxy; BMG Labtechnologies). For UV irradiation experiments, we grew cells harboring plasmid pL(*lexO*)-*gfp* as described in the legend to Fig. 1. At an OD_{600} of 0.5 to 0.6, we transferred 1 ml of the culture to a 100-mm petri dish and irradiated the cultures with 10^4 μJ/cm^2 UV light inside a UVC 500 cross-linker (Hoefer) for 4 s. Then, we placed 250-μl samples into each well of a 96-well plate. We measured fluorescence (fluorescence units [FU]) with a fluorometer over a period of 4 h. All of the values shown are relative to those of control cells not irradiated with UV.

DNA fragmentation assay using FACS analysis. DNA fragmentation was detected by the terminal deoxynucleotidyltransferase-mediated dUTP-biotin nick end labeling (TUNEL) assay (46). To perform the TUNEL assay, we used the Apo-Direct kit and detected fluorescence in individual DNA fragmented cells by flow cytometry as we have previously described (10). We determined the intensity of the fluorescence by fluorescence-activated cell sorting (FACS) analysis using the LSRII FACS machine and FCS Express V3 software, as we have described previously (10).

Determining RNA integrity. To detect RNA degradation, we grew cells and treated them with the appropriate materials as described above. We extracted RNA using RNAprotect bacterial reagent (Qiagen) and the RNeasy minikit (Qiagen) combined with the RNase-free DNase set (Qiagen) according to the manufacturer's instructions. To determine RNA integrity, we analyzed RNA samples (200 to 400 ng) using an Agilent Technology 2100 Bioanalyzer.

Microarray analysis. For microarray analysis, cells were grown, incubated with antibiotics, and washed as described above. RNA extraction was carried out as described above. The RNA was subjected to cDNA synthesis, fragmentation, and end terminus biotin labeling according to the standard Affymetrix prokaryotic GeneChip expression protocol with the following modifications: cDNA synthesis was performed with SuperScript III reverse transcriptase (Molecular Probes, Invitrogen [Carlsbad, CA, USA]), and cDNA reaction mixtures were incubated at 42°C overnight. Finally, labeled cDNA samples were hybridized to Affymetrix GeneChip *E. coli* arrays. Hybridized arrays were stained and washed using the Affymetrix Fuidic Station 450. After staining, arrays were scanned with a GC3000 scanner. For CEL file generation, we used the Affymetrix GeneChip Command Console software (AGCC).

Statistics for microarray analysis. Robust multiarray average (RMA) normalization was performed on CEL files using the Partek Genomic Suite 6.5. Additional statistical analysis was carried out using the Spotfire software package (Somerville, MA, USA) and custom MatLab (R2010B) routines. Gene selection was done using the false discovery rate (FDR) correction procedure for adjusting genes with P values smaller than 0.05 and fold changes greater than 2.

Real-time PCR. For real-time PCR analysis, cells were grown, incubated with antibiotics, and washed as described above. RNA extraction was carried out as described above. cDNA was synthesized by using the ProtoScript Moloney murine leukemia virus (M-MuLV) first-strand cDNA synthesis kit (New England Biolabs) with random primers (kit component). *idnT* RNA transcript levels were used as an endogenous control for RNA levels in the samples. To amplify *dinB* cDNA, the following primers were used: forward primer GAGCGTAGTCAGGGGATTGA and reverse primer TCGCTTCACATTCAGACCAG. To amplify *umuC* cDNA, the following primers were used: forward primer GCTTTACGCA GACATGAGCA and reverse primer CGCAGAATGCCTCATCAATA. To amplify *idnT* cDNA, the following primers were used: forward primer

GTGGGTTTTGTCCTGCTGTT and reverse primer ACAGAGAGCGCT GCTACCAT. Real-time analysis was than conducted using Fast SYBR Green master mix (Applied Biosystems) in a 7500 Fast real-time PCR system (Applied Biosystems).

Membrane depolarization assays using FACS analysis. Cells were grown, incubated with antibiotics, and washed as described above. Samples were diluted 1:100 in PBS (pH 7.2). To stain the cells, we added 1 μl $DiBAC_4$ (1 mg/ml in ethanol) to 1 ml of the diluted cells and incubated them at room temperature for 15 min. To analyze the intensity of the $DiBAC_4$ fluorescence, we used an LSRII FACS machine as we have described previously (10).

Detection of $OH^{\cdot}$ formation. To detect $OH^{\cdot}$, we used the molecule hydroxyphenyl fluorescein (HPF), which fluoresces only when it reacts with $OH^{\cdot}$. We grew the cells, treated them, and washed them twice with PBS (pH 7.2) as described above. Then, we added HPF to the samples to a final concentration of 10 μM and incubated the cells, protected from light, at room temperature for 1 h, after which we washed them twice with PBS (pH 7.2). We analyzed them for staining intensity using an LSRII FACS machine with a 488-nm argon laser for excitation and a 530- $\pm$ 15-nm emission filter; we analyzed the results using FCS Express V3 software.

Quantifying LexA degradation by Western blot analysis. We grew cells in 10 ml M9 minimal medium, as described above, and treated them with various concentrations of NA for different periods of time as described in the figure legends. To lyse the cells, we centrifuged samples for 2 min and then suspended the cell pellets in 50 μl of Bugbuster master mix (Novagen), incubating them with vigorous shaking at room temperature for 10 min. Then, we centrifuged them at 4°C for 10 min and transferred the supernatants containing the crude extract to fresh tubes. We determined protein concentrations using the Bradford assay (Bio-Rad, Hercules, CA, USA). For Western blot analysis, we used rabbit polyclonal antibody to the LexA DNA binding region as the primary antibody (Abcam) and donkey polyclonal antibody to rabbit IgG (horseradish peroxidase [HRP]) as the secondary antibody (Abcam).

Measuring enzyme activities. We grew cells to an OD_{600} of 0.5, treated them with NA at the indicated concentrations, incubated them for the indicated times, and collected them by centrifugation. To lyse the cells, we suspended them in 50 mM morpholineethanesulfonic acid (MES) buffer (pH 6.0) with 10% glycerol and 1 mg/ml lysozyme and incubated them with vigorous shaking at room temperature for 5 min; we then sonicated them, for 10 s, twice at 30-s intervals. We froze aliquots of whole-cell extracts in liquid N2 medium stored at −80°C. We measured complex II activity as the succinate dehydrogenase (SDH) activity based on the succinate-mediated phenazine methosulfate reduction of dichloroindophenol at 600 nm as described previously (47). We measured complex I activity as deamino-NADH dehydrogenase activity by monitoring the reduction of deamino-NADH at 340 nm as described previously (47). We measured NADH dehydrogenase II activity by monitoring the general reduction of NADH at 340 nm and by reducing the activity of deamino-NADH dehydrogenase activity from the total NADH dehydrogenase activity.

Microarray data accession number. All CEL files are available from GEO under accession number GSE56251.

SUPPLEMENTAL MATERIAL

Supplemental material for this article may be found at http://mbio.asm.org/lookup/suppl/doi:10.1128/mBio.01426-14/-/DCSupplemental.

Figure S1, PDF file, 0.1 MB.
Figure S2, PDF file, 0.1 MB.
Figure S3, PDF file, 0.2 MB.
Figure S4, PDF file, 0.1 MB.
Figure S5, PDF file, 0.2 MB.
Figure S6, PDF file, 0.1 MB.
Figure S7, PDF file, 0.1 MB.
Figure S8, PDF file, 0.1 MB.
Figure S9, PDF file, 0.1 MB.
Table S1, DOC file, 0.2 MB.

ACKNOWLEDGMENTS

This research was supported by the Israel Science Foundation (ISF) (grant 66/10) and the United States Army (grant W911NF-13-1-0371).

We thank F. R. Warshaw-Dadon (Jerusalem, Israel) for her critical reading of the manuscript.

REFERENCES

1. **Yuan J, Kroemer G.** 2010. Alternative cell death mechanism in development and beyond. Genes Dev. **24:**2592–2602. http://dx.doi.org/10.1101/gad.1984410.
2. **Hengartner MO.** 2000. The biochemistry of apoptosis. Nature **407:**770–776. http://dx.doi.org/10.1038/35037710.
3. **Jacobson MD, Weil M, Raff MC.** 1997. Programmed cell death in animal development. Cell **88:**347–354. http://dx.doi.org/10.1016/S0092-8674(00)81873-5.
4. **Nagata S.** 1997. Apoptosis by death factor. Cell **88:**355–365. http://dx.doi.org/10.1016/S0092-8674(00)81874-7.
5. **Hockenbery DM, Oltvai ZN, Yin XM, Milliman CL, Korsmeyer SJ.** 1993. Bcl-2 functions in an antioxidant pathway to prevent apoptosis. Cell **75:**241–251. http://dx.doi.org/10.1016/0092-8674(93)80066-N.
6. **Kerr JF, Wyllie AH, Currie AR.** 1972. Apoptosis: a basic biological phenomenon with wide-ranging implications in tissue kinetics. Br. J. Cancer **26:**239–257.
7. **Li P, Nijhawan D, Budihardjo I, Srinivasula SM, Ahmad M, Alnemri ES, Wang X.** 1997. Cytochrome *c* and dATP-dependent formation of Apaf-1/caspase-9 complex initiates an apoptotic protease cascade. Cell **91:**479–489. http://dx.doi.org/10.1016/S0092-8674(00)80434-1.
8. **Wyllie AH.** 1980. Glucocorticoid-induced thymocyte apoptosis is associated with endogenous endonuclease activation. Nature **284:**555–556. http://dx.doi.org/10.1038/284555a0.
9. **Aizenman E, Engelberg-Kulka H, Glaser G.** 1996. An *Escherichia coli* chromosomal "addiction module" regulated by guanosine (corrected) 3′,5′-bispyrophosphate: a model for programmed bacterial cell death. Proc. Natl. Acad. Sci. U. S. A. **93:**6059–6063. http://dx.doi.org/10.1073/pnas.93.12.6059.
10. **Erental A, Sharon I, Engelberg-Kulka H.** 2012. Two programmed cell death systems in *Escherichia coli*: an apoptotic-like death is inhibited by the *mazEF* mediated death pathway. PLoS Biol. **10:**e1001281. http://dx.doi.org/10.1371/journal.pbio.1001281.
11. **Godoy VG, Jarosz DF, Walker FL, Simmons LA, Walker GC.** 2006. Y-family DNA polymerases respond to DNA damage-independent inhibition of replication fork progression. EMBO J. **25:**868–879. http://dx.doi.org/10.1038/sj.emboj.7600986.
12. **Hazan R, Sat B, Engelberg-Kulka H.** 2004. *Escherichia coli mazEF*-mediated cell death is triggered by various stressful conditions. J. Bacteriol. **186:**3663–3669. http://dx.doi.org/10.1128/JB.186.11.3663-3669.2004.
13. **Sat B, Reches M, Engelberg-Kulka H.** 2003. The *Escherichia coli mazEF* suicide module mediates thymineless death. J. Bacteriol. **185:**1803–1807. http://dx.doi.org/10.1128/JB.185.6.1803-1807.2003.
14. **Zhang Y, Zhang J, Hoeflich KP, Ikura M, Qing G, Inouye M.** 2003. MazF cleaves cellular mRNAs specifically at ACA to block protein synthesis in *Escherichia coli*. Mol. Cell **12:**913–923. http://dx.doi.org/10.1016/S1097-2765(03)00402-7.
15. **Vesper O, Amitai S, Belitsky M, Byrgazov K, Kaberdina AC, Engelberg-Kulka H, Moll I.** 2011. Selective translation of leaderless mRNAs by specialized ribosomes generated by MazF in *Escherichia coli*. Cell **147:**147–157. http://dx.doi.org/10.1016/j.cell.2011.07.047.
16. **Amitai S, Kolodkin-Gal I, Hananya-Meltabashi M, Sacher A, Engelberg-Kulka H.** 2009. *Escherichia coli* MazF leads to the simultaneous selective synthesis of both "death proteins" and "survival proteins." PLoS Genet. **5:**e1000390. http://dx.doi.org/10.1371/journal.pgen.1000390.
17. **Hersh MN, Ponder RG, Hastings PJ, Rosenberg SM.** 2004. Adaptive mutation and amplification in *Escherichia coli*: two pathways of genome adaptation under stress. Res. Microbiol. **155:**352–359. http://dx.doi.org/10.1016/j.resmic.2004.01.020.
18. **Little JW.** 1991. Mechanism of specific LexA cleavage: autodigestion and the role of RecA coprotease. Biochimie **73:**411–421.
19. **Radman M.** 1975. SOS repair hypothesis: phenomenology of an inducible DNA repair which is accompanied by mutagenesis. Basic Life Sci. **5A:**355–367.

20. **Sutton MD, Smith BT, Godoy VG, Walker GC.** 2000. The SOS response: recent insights into *umuDC*-dependent mutagenesis and DNA damage tolerance. Annu. Rev. Genet. **34:**479–497. http://dx.doi.org/10.1146/annurev.genet.34.1.479.
21. **Walker G.** 1996. The SOS response of *Escherichia coli*, p 1400–1416. *In* Neidhardt FC, Curtiss R, III, Ingraham JL, Lin ECC, Low KB, Magasanik B, Reznikoff WS, Riley M, Schaechter M, Umbarger HE (ed), *Escherichia coli* and *Salmonella*: cellular and molecular biology, vol **1**, 2nd ed, vol **1**. ASM Press, Washington, DC.
22. **Courcelle J, Khodursky A, Peter B, Brown PO, Hanawalt PC.** 2001. Comparative gene expression profiles following UV exposure in wild-type and SOS-deficient *Escherichia coli*. Genetics **158:**41–64.
23. **Fernández De Henestrosa AR, Ogi T, Aoyagi S, Chafin D, Hayes JJ, Ohmori H, Woodgate R.** 2000. Identification of additional genes belonging to the LexA regulon in *Escherichia coli*. Mol. Microbiol. **35:**1560–1572. http://dx.doi.org/10.1046/j.1365-2958.2000.01826.x.
24. **Little JW.** 1984. Autodigestion of lexA and phage lambda repressors. Proc. Natl. Acad. Sci. U. S. A. **81:**1375–1379. http://dx.doi.org/10.1073/pnas.81.5.1375.
25. **Davies BW, Kohanski MA, Simmons LA, Winkler JA, Collins JJ, Walker GC.** 2009. Hydroxyurea induces hydroxyl radical-mediated cell death in *Escherichia coli*. Mol. Cell **36:**845–860. http://dx.doi.org/10.1016/j.molcel.2009.11.024.
26. **Cashel M, Gentry DR, Hernandez VZ, Vinella D.** 1996. The stringent response, p -1458–1496. *In* Neidhardt FC, Curtiss R, III, Ingraham JL, Ling ECC, Low KB, Magasanik B, Reznikoff WR, Riley M, Schaechter M, Umbarger HE (ed), *Escherichia coli* and *Salmonella*: cellular and molecular biology, vol **1**, 2nd ed, vol **1**. ASM Press, Washington, DC.
27. **Metzger S, Schreiber G, Aizenman E, Cashel M, Glaser G.** 1989. Characterization of the *relA* mutation and a comparison of *relA1* with new *relA* null alleles in *Escherichia coli*. J. Biol. Chem. **264:**21146–21152.
28. **Degen WG, Pruijn GJ, Raats JM, van Venrooij WJ.** 2000. Caspase-dependent cleavage of nucleic acids. Cell Death Differ. **7:**616–627. http://dx.doi.org/10.1038/sj.cdd.4400672.
29. **Mroczek S, Kufel J.** 2008. Apoptotic signals induce specific degradation of ribosomal RNA in yeast. Nucleic Acids Res. **36:**2874–2888. http://dx.doi.org/10.1093/nar/gkm1100.
30. **Jacob AI, Köhrer C, Davies BW, RajBhandary UL, Walker GC.** 2013. Conserved bacterial RNase YbeY plays key roles in 70S ribosome quality control and 16S rRNA maturation. Mol. Cell **49:**-427–438. http://dx.doi.org/10.1016/j.molcel.2012.11.025.
31. **Little JW, Edmiston SH, Pacelli LZ, Mount DW.** 1980. Cleavage of the *Escherichia coli* lexA protein by the recA protease. Proc. Natl. Acad. Sci. U. S. A. **77:**3225–3229. http://dx.doi.org/10.1073/pnas.77.6.3225.
32. **Rapisarda VA, Chehín RN, De Las Rivas J, Rodríguez-Montelongo L, Farías RN, Massa EM.** 2002. Evidence for Cu(I)-thiolate ligation and prediction of a putative copper-binding site in the *Escherichia coli* NADH dehydrogenase-2. Arch. Biochem. Biophys. **405:**87–94. http://dx.doi.org/10.1016/S0003-9861(02)00277-1.
33. **Simon HU, Haj-Yehia A, Levi-Schaffer F.** 2000. Role of reactive oxygen species (ROS) in apoptosis induction. Apoptosis **5:**415–418. http://dx.doi.org/10.1023/A:1009616228304.
34. **Ricci JE, Muñoz-Pinedo C, Fitzgerald P, Bailly-Maitre B, Perkins GA, Yadava N, Scheffler IE, Ellisman MH, Green DR.** 2004. Disruption of mitochondrial function during apoptosis is mediated by caspase cleavage of the p75 subunit of complex I of the electron transport chain. Cell **117:**773–786. http://dx.doi.org/10.1016/j.cell.2004.05.008.
35. **Schwartz J, Djaman O, Imlay JA, Kiley PJ.** 2000. The cysteine desulfurase, IscS, has a major role in in vivo Fe-S cluster formation in *Escherichia coli*. Proc. Natl. Acad. Sci. U. S. A. **97:**9009–9014. http://dx.doi.org/10.1073/pnas.160261497.
36. **Bayles KW.** 2014. Bacterial programmed cell death: making sense of a paradox. Nat. Rev. Microbiol. **12:**63–69. http://dx.doi.org/10.1038/nrmicro3136.
37. **Dwyer DJ, Camacho DM, Kohanski MA, Callura JM, Collins JJ.** 2012. Antibiotic-induced bacterial cell death exhibits physiological and biochemical hallmarks of apoptosis. Mol. Cell **46:**561–572. http://dx.doi.org/10.1016/j.molcel.2012.04.027.
38. **Kolodkin-Gal I, Sat B, Keshet A, Engelberg-Kulka H.** 2008. The communication factor EDF and the toxin–antitoxin module *mazEF* determine the mode of action of antibiotics. PLoS Biol. **6:**e319. http://dx.doi.org/10.1371/journal.pbio.0060319.
39. **Belitsky M, Avshalom H, Erental A, Yelin I, Kumar S, London N, Sperber M, Schueler-Furman O, Engelberg-Kulka H.** 2011. The *Escherichia coli* extracellular death factor EDF induces the endoribonucleolytic activities of the toxins MazF and ChpBK. Mol. Cell **41:**625–635. http://dx.doi.org/10.1016/j.molcel.2011.02.023.
40. **Bos J, Yakhnina AA, Gitai Z.** 2012. BapE DNA endonuclease induces an apoptotic-like response to DNA damage in *Caulobacter*. Proc. Natl. Acad. Sci. U. S. A. **109:**18096–18101. http://dx.doi.org/10.1073/pnas.1213332109.
41. **Pagliarini DJ, Calvo SE, Chang B, Sheth SA, Vafai SB, Ong SE, Walford GA, Sugiana C, Boneh A, Chen WK, Hill DE, Vidal M, Evans JG, Thorburn DR, Carr SA, Mootha VK.** 2008. A mitochondrial protein compendium elucidates complex I disease biology. Cell **134:**112–123. http://dx.doi.org/10.1016/j.cell.2008.06.016.
42. **Green DR.** 2011. Means to an end: apoptosis and other cell death mechanisms, p 111–126. Cold Spring Harbor Laboratory Press, New York, NY.
43. **Carmona-Gutierrez D, Kroemer G, Madeo F.** 2012. When death was young: an ancestral apoptotic network in bacteria. Mol. Cell **46:**552–554. http://dx.doi.org/10.1016/j.molcel.2012.05.032.
44. **Engelberg-Kulka H, Reches M, Narasimhan S, Schoulaker-Schwarz R, Klemes Y, Aizenman E, Glaser G.** 1998. *rexB* of bacteriophage lambda is an anti-cell death gene. Proc. Natl. Acad. Sci. U. S. A. **95:**15481–15486. http://dx.doi.org/10.1073/pnas.95.26.15481.
45. **Datsenko KA, Wanner BL.** 2000. One-step inactivation of chromosomal genes in *Escherichia coli* K-12 using PCR products. Proc. Natl. Acad. Sci. U. S. A. **97:**6640–6645. http://dx.doi.org/10.1073/pnas.120163297.
46. **Gavrieli Y, Sherman Y, Ben-Sasson SA.** 1992. Identification of programmed cell death in situ via specific labeling of nuclear DNA fragmentation. J. Cell Biol. **119:**493–501. http://dx.doi.org/10.1083/jcb.119.3.493.
47. **Ezraty B, Vergnes A, Banzhaf M, Duverger Y, Huguenot A, Brochado AR, Su SY, Espinosa L, Loiseau L, Py B, Typas A, Barras F.** 2013. Fe-S cluster biosynthesis controls uptake of aminoglycosides in a ROS-less death pathway. Science **340:**1583–1587. http://dx.doi.org/10.1126/science.1238328.